Dispersion Polymerization of Methyl Methacrylate in Supercritical CO_2

Carole Lepilleur and Eric J. Beckman*

Chemical Engineering Department, University of Pittsburgh, 1249 Benedum Hall, Pittsburgh, Pennsylvania 15261

Received May 28, 1996; Revised Manuscript Received November 26, 1996[⊗]

ABSTRACT: A series of graft copolymers, poly(methyl methacrylate-*co*-hydroxyethyl methacrylate)-*g*-poly(perfluoropropylene oxide), was synthesized for application as stabilizers in dispersion polymerization of methyl methacrylate in supercritical carbon dioxide. The backbone, poly(methyl methacrylate-*co*-hydroxyethyl methacrylate), is effectively insoluble in carbon dioxide and the grafted chains, poly(perfluoropropylene oxide), are completely miscible in carbon dioxide at moderate pressures. The effect of molecular architecture on polymerization rate and PMMA particle size was evaluated by varying the molecular weight of the anchor group (backbone of the copolymer), molecular weight of the CO_2-soluble graft chain, and graft chain density. The efficiency of the graft copolymers as dispersants was demonstrated as micron-size polymer beads of molecular weight greater than 100 000 were produced. The results showed that a careful balance between anchor group size (backbone length) and amount of soluble component (either graft chain length or graft chain density) is necessary but not sufficient to achieve adequate stabilization and that the distribution of the soluble component along the anchor group was also important. Furthermore, the backbone molecular weight was shown as the key component for stabilization, provided that enough CO_2-philic component has been included to ensure solubility.

Introduction

Supercritical fluids (SCFs) have been used in a wide range of processes,[1−4] including polymerization media.[5−10] Carbon dioxide is often used in SCF processes because it is readily available, nonflammable, nontoxic, and inexpensive. Further, CO_2 is one of the few organic solvents which is not regulated as a VOC (volatile organic compound) by the U.S. EPA. It has a relatively low critical temperature (T_c = 31.1 °C) and a moderate critical pressure (P_c = 72 bar). As with all SCFs, CO_2 offers mass transfer advantages over conventional solvents because of its low viscosity and surface tension, but it is a poor solvent for most polymers of high molecular weight, whether polar or nonpolar.[11] Unfortunately, typical dispersants (alkyl copolymers) exhibit poor to negligible solubility in CO_2, preventing application of dispersion polymerization in this environmentally-benign solvent. CO_2 is a low dielectric solvent and calculations would suggest that the solubility parameter for CO_2 approaches that for conventional liquid alkanes at pressures above 300 bars, but structure-solubility results from the literature would suggest that the solvent properties of CO_2 are quite different from that of ordinary alkanes.[12,13] As shown by Johnston et al.,[14] the calculated solubility parameter for CO_2 is inflated by approximately 20% by the strong quadropole moment of CO_2. Factors that contribute to favorable interactions with CO_2 are low polarizability, low solubility parameter, and electron donating capability, given that CO_2 is a weak Lewis acid. Consequently, one would expect CO_2 to be a good solvent for those materials with solubility parameters in the 4−5 $(cal/cm^3)^{0.5}$ range, such as fluoroethers, fluoroalkanes, fluoroacrylates, and siloxanes. Indeed, results from the literature confirm this.[12,13,15−22]

In order to successfully perform dispersion polymerizations, we require dispersing aids (graft or block copolymers) which are highly CO_2-soluble, yet will interact with the growing polymer in a thermodynamically favorable manner. DeSimone et al.[16−18] have employed fluoroacrylate homopolymers and fluoroacrylate−styrene copolymers for dispersing agents in dispersion polymerization in CO_2. They showed that AIBN was active in CO_2 and could efficiently initiate free radical polymerization.[17] The authors then performed free radical dispersion polymerization of methyl methacrylate in supercritical CO_2.[16,18] They demonstrated that using poly(1,1-dihydroperfluorooctyl acrylate) (poly(FOA)) as dispersant could effectively stabilize the dispersion. The successful formation of a stable colloid in supercritical CO_2 resulted in high polymerization rates and high molecular weight polymer. They also showed that increasing the dispersant concentration led to smaller and more uniform particles, and increasing the overall molecular weight of the stabilizer resulted in increasing the particle size. Further work by Hsiao et al.[27] showed that use of poly(FOA) (0.25−17 wt %) allowed a 90% yield of PMMA in 4 h at 65 °C and 345 bar, that the molecular weight of the PMMA was relatively insensitive to the amount of poly(FOA) employed or the pressure, provided that the pressure was maintained above the solubilization threshold of the Poly(FOA). The size of the PMMA beads generated ranged from 2.5 to 1.5 μm, with polydispersities as low as 1.01. Recently, Shaffer and co-workers[28] employed a reactive dispersant, a silicone macromonomer, to perform dispersion polymerization of MMA in CO_2 at 65 °C and 340 bar. Results were generally similar to those reported by Hsiao, except that higher amounts of dispersant were required to achieve small, monodisperse particles. Shaffer found that a significant portion of the silicone macromonomer was covalently incorporated into the polymer beads.

The stabilizers that we designed for dispersion polymerization of MMA in supercritical CO_2 are poly(methyl methacrylate-*co*-hydroxyethyl methacrylate-*g*-poly(perfluoropropylene oxide)), where the backbone or anchor group, poly(methyl methacrylate-*co*-hydroxyethyl methacrylate), is poorly miscible with CO_2 and will have an affinity for the forming polymer (poly(methyl methacrylate)). The graft chains or soluble component, consisting

[⊗] Abstract published in *Advance ACS Abstracts,* February 1, 1997.

S0024-9297(96)00764-4 CCC: $14.00

PROPOSED COMB-LIKE DISPERSANT:

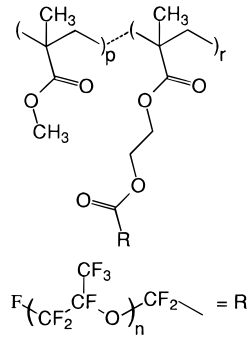

Figure 1. Chemical structure of the graft copolymer dispersant.

of poly(perfluoropropylene oxide), are very soluble in CO_2 at low pressure and are attached to the particle through the anchor component. Fluorinated compounds show the highest affinity for CO_2 due to their low dipolarity/polarizability parameter.[21,23,24] Fluoroethers have a low solubility parameter 4−5 $(cal/cm^3)^{0.5}$. Since the solubility parameter of CO_2 is 5.5−6 $(cal/cm^3)^{0.5}$ at 293 K over the 800−900 kg/m^3 range, these compounds are miscible. Additionally, the oxygen in the perfluoropropylene oxide repeat unit has an electron-donor capacity that enhances miscibility with the Lewis acid CO_2.[24] Taking into account all these factors, the graft copolymer dispersant will contain highly CO_2-philic graft chains and a polymeric backbone that will show affinity with the dispersed polymer formed during polymerization. The chemical structure of the graft copolymer dispersant is illustrated in Figure 1. The anchor group molecular weight and the molecular weight and density (graft chain density) of the soluble component were each varied during this study.

Experimental Section

Materials. All reagents and solvents used in the work described herein were purchased from Aldrich and used as received, unless otherwise specified.

Synthesis of Poly(MMA$_x$-*co*-HEMA$_y$). A 1.0 L three-neck round bottom flask equipped with a condenser and a thermometer was charged with 500 mL of ethanol and heated to 70 °C under a nitrogen atmosphere. The monomers, methyl methacrylate (MMA) and hydroxyethyl methacrylate (HEMA), having been previously distilled under vacuum (10 mmHg) at 60−65 and 90−95 °C, respectively, were added along with butanethiol to the reactor in various amounts. After temperature re-equilibration, 2,2′-azobis(isobutyronitrile) (AIBN) (Kodak), having been recrystallized from acetone and dissolved in 20 mL of ethanol, was injected. The mixture was stirred for 12 h. The resulting polymer was precipitated into petroleum ether, redissolved in chloroform and reprecipitated into petroleum ether. The powder was dried in a vacuum oven (10 mmHg) at 60 °C for several days.

IR (KBr): 3535, 2997, 2947, 1736, 1483, 1388, 1240, 1080, 987, 912, 844, 750 cm^{-1}. ^{1}H-NMR (300 MHz, $CDCl_3$): δ 4.12 (m, 2H), 3.85 (m. 2H), 3.6 (s, 3H), 1.93 (m, 2H), 1.85 (m, 2H), 1.4−1.22 (m, 3H), 1.04−0.85 (m, 3H) ppm.

Synthesis of Acid Chloride Terminated Poly(perfluoropropylene oxide). A 250 mL three-neck round bottom flask equipped with a condenser and a thermometer was charged with 100 g (4.0×10^{-2} mol) of carboxylic acid terminated poly(perfluoropropylene oxide) of low molecular weight ($M_n = 2.5 \times 10^3$) (Miller-Stefenson) and 100 g of methylperfluorocyclohexane. The mixture was heated to reflux (75 °C) under a nitrogen blanket. Thionyl chloride (6 mL, 6.0×10^{-2} mol) and dimethylformamide (DMF) (3.2 mL, 4.0×10^{-2} mol) were slowly added. The reaction mixture was left stirring for 8 h. The system was placed under vacuum on a rotary evaporator so as to remove methylperfluorocyclohexane. The residual thionyl chloride and DMF were separated with the aid of a separatory funnel.

IR (neat): 1809, 1456, 1250−1050, 985, 808, 750 cm^{-1}. ^{1}H-NMR (300 MHz, 1,1,3-trichlorotrifluoroethane): no peaks.

The same procedure was followed when using carboxylic acid terminated poly(perfluoropropylene oxide) of middle and high molecular weights ($M_n = 5.0 \times 10^3$ and 7.5×10^3, respectively). The appropriate amounts of thionyl chloride and DMF were employed.

Synthesis of the Graft Copolymer. A 500 mL three-neck round bottom flask equipped with a condenser, a thermometer, and an addition funnel was purged with nitrogen and charged with 1.0 g of poly(MMA$_x$-*co*-HEMA$_y$) that had been previously dissolved in 120 mL of a 1:1 mixture of THF and 1,1,2-trichlorotrifluoroethane. To this was added an excess of a polymer-supported (dialkylamino)pyridine catalyst (poly-DMAP, Reillex Industries). The acid chloride terminated poly(perfluoropropylene oxide) (1.5 equiv of acid chloride per hydroxyl), having been previously dissolved in 100 mL of 1,1,2-trichlorotrifluoroethane, was added dropwise to the vigorously stirred mixture. The reaction mixture was left at 50 °C for 7 days, after which time the polyDMAP was filtered off. The solvents were removed under reduced pressure (10 mmHg) on a rotary evaporator.

IR (neat): 2995, 2953, 1784, 1734, 1450, 1250−1050, 1087, 997, 904, 810, 750 cm^{-1}. ^{1}H-NMR (300 MHz, 1,1,3-trichlorotrifluoroethane): δ 4.58 (m, 2H), 4.27 (m, 2H), 3.6 (s, 3H), 2.11−1.89 (m, 4H), 1.10−0.90 (m, 6H) ppm.

The samples' chemical integrities were periodically checked by FTIR, and the spectra showed no signs of hydrolysis after several months of storage.

It is difficult to determine the extent of reaction of the pendant hydroxy groups of the copolymer and the PFPO−acid chloride by ^{1}H-NMR, because the strong methyl peak of MMA (present in the backbone of the copolymer) overlaps with the methylene peaks (CH_2CH_2O) of the HEMA comonomer. In order to gauge the extent of reaction, a model reaction has been performed: that between PFPO−acid chloride and HEMA (hydroxyethyl methacrylate). The reaction was performed under the exact same conditions as for the graft copolymer synthesis. In using HEMA, we eliminate the strong methyl peak of MMA (present in the graft copolymer ^{1}H-NMR spectrum) and thus the overlapping peaks. ^{19}F-NMR has also been performed on PFPO−carboxylic acid, PFPO−acid chloride, and PFPO−HEMA (as model compound). Using ^{1}H-NMR, the extent of the model reaction was easy to determine by integrating the ^{1}H-NMR peaks of the methylene groups adjacent to the alcohol or ester groups. After reaction, the two methylene group signals shift from 3.92 and 4.25 to 4.42 and 4.61 ppm, respectively. Additionally, in the ester spectrum, no remaining peaks at 3.92 and 4.25 ppm were detected, suggesting near 100% conversion of the alcohol group into an ester linkage, in the model reaction. On the other hand, no differences in the ^{19}F-NMR spectra were observed for the three compounds mentioned. Although extents of reaction on polymers are typically lower than in analogous small molecule systems, because the polymer reactions were conducted under homogeneous conditions, these results suggest greater than 90% conversion in the polymer system.

Dispersion Polymerization in SCFs. The reactor is made of a single piece of stainless steel with an internal volume of ca. 55 mL, into which are cut two opposed view windows designed to fit 1 in. diameter sapphire windows. The body of the reactor has three ports to the internal chamber and four ports into the wall design to accommodate the heating elements. The lid of the reactor is fitted with a high-pressure magnetic stirrer mix head (Parr Instrument Co.) which can rotate at speeds as high as 600 rpm. The mixing shaft of the stirrer is fitted with three equally spaced turbine propellers. The reactor temperature is controlled using a 2001TC-AT PID controller (Omega Inc.) in connection with an iron−constantan thermocouple placed in the lowest of the three reactor chamber ports. A 280E pressure transducer (Setra Systems Inc.) is connected in line with a rupture disk (High Pressure Equipment Co.) to a nonisolatable line from the reactor. The

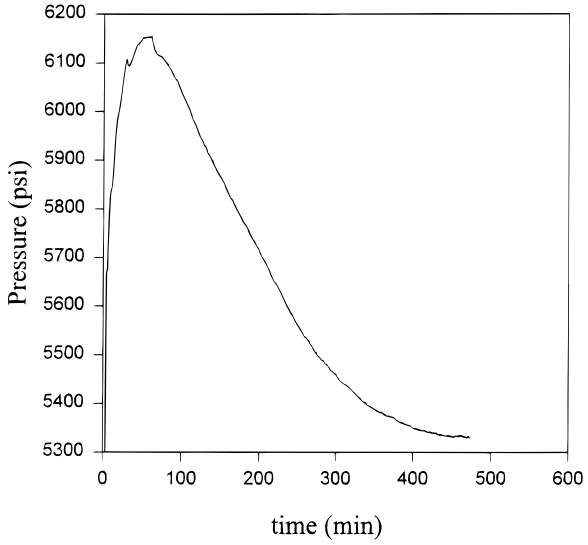

Figure 2. Pressure change monitored during dispersion polymerization at 65 °C.

transducer is connected to a 500 LED readout (Wavetek Corp.). The pressure and temperature are recorded every second, and the stored values are the averages operated every minute, through a Metrabyte acquisition board.

For the dispersion polymerizations, the reactor was charged with 10 g (ca. 23 wt %, 2.2 mmol/L of CO_2) of freshly distilled MMA (60−65 °C and 10 mmHg), an appropriate amount of graft copolymer poly(MMA_x-*co*-$HEMA_y$)-*g*-perfluoropoly(propylene oxide), and 50 mg (5 mmol) of AIBN. The reactor was flushed with CO_2, heated to 65 °C, and pressurized to 380 bar. The reaction mixture was vigorously stirred (V = 400 rpm) for as long as the pressure in the reactor continued to change—once pressure remained constant for a period of 30 min, the reaction was stopped. In general, running the reaction until the pressure leveled out led to production of over 9 g of polymer from 10 g of monomer; thus the yield in our polymerizations was always over 90%, although it was difficult to quantify yield owing to loss of polymer in the high-pressure lines. However, given that the rate of polymerization varied with changing dispersant architecture and pressure, reactions were therefore run for times ranging from just over 3 to up to 10 h. At the beginning of the reaction, the reaction medium is clear, indicating miscibility of the reactants with CO_2. After approximately 20−30 min, cloudiness slowly appears until the reaction medium becomes totally opaque, indicating the formation of the PMMA, which is insoluble in CO_2. The pressure of the reactor decreased in a steady manner after equilibration of the temperature, with a total pressure drop that averaged 50 bar (Figure 2). At the end of the reaction, the reactor was cooled to 20 °C and depressurized by venting of the CO_2, leaving a dry polymer powder.

IR (film): 3437, 2951, 1734, 1456, 1240, 1147, 987, 912, 842 cm^{-1}. ^{1}H-NMR ($CDCl_3$, 300 MHz): δ 3.61 (s, 3H), 1.81 (m, 2H), 1.02−1.85 ppm (m, 3H).

Compressibility Measurements. A high-pressure variable volume view cell was used to measure the compressibility of both monomer and polymer and their mixtures at 65 °C. The cell was charged with predetermined amounts of materials and CO_2 which duplicate the concentrations present in the reactor during polymerization. In order to simulate the various stages of the polymerization the choice of charging materials was either 100% monomer (initial conditions), 100% polymer (final conditions), or a mixture of the two (intermediate stages). The cell volume was recorded over a range of pressures. The changes in volume with pressure for each case were plotted against pressure. The compressibility terms (dV/dP) were derived from these pressure/volume measurements and are plotted against pressure.

Characterization. Gel permeation chromatography (GPC) (Waters model 150 CV) was used to determine molecular weight averages and the polydispersity index of the poly(MMA_x-*co*-$HEMA_y$) copolymers. The instrument is equipped with a differential viscometer downstream of two columns (Styragel, pores sizes 500 and 1000 Å, Millipore) which are placed in series. Tetrahydrofuran (THF) was used as the mobile phase solvent at a flow rate of 1 mL/min. Peak molecular weights were estimated on the basis of 18 monodispersed polystyrene (PS) standards (Millipore), covering molecular weights ranging from 1.6×10^2 to 1.6×10^5.

Scanning electron microscopy (SEM) (Topcon DS130) was used to determine particle size and distribution of PMMA. Samples were redispersed onto copper tape and coated with gold prior to analysis.

Theory: Analysis of Pressure Changes during Polymerization Reactions

It has been previously observed that the pressure can change significantly (both increasing and decreasing) during a polymerization of a vinyl monomer in a supercritical fluid. Hsiao and colleagues noticed that the pressure decreased during dispersion polymerization of MMA at high initial pressures (greater than 300 bar), while rising during polymerization when the initial pressure was lower. That pressure changes during polymerization is not surprising, in that the molar volume of a vinyl monomer is usually higher than that of the subsequent polymer—the volume change upon polymerization is the basis for the use of dilatometry[30] to determine the rate of polymerization in conventional liquid systems. In our constant volume, high-pressure reactors, the change of volume upon polymerization prompts a change in pressure. However, we must also be cognizant that as the composition of the system changes, the volume change on mixing for each phase (which accounts for nonideal mixing behavior) in the system can also change. Thus, although one might expect that the pressure should always decrease upon polymerization (owing to the volume decrease upon polymerizing a vinyl monomer), the variation of the nonideal contributions with pressure and composition could conceivably lead to pressure increases, as will be shown below.

For the dispersion polymerization of MMA in CO_2, we have two phases, I and II, where phase I consists of carbon dioxide and monomer (components 1 and 2 in phase I), while phase II contains CO_2, monomer, and polymer repeat units (components 1, 2, and 3 in phase II). That no polymer is present in phase I is a reasonable approximation, in that previous work has shown that high molecular weight poly(methyl methacrylate) exhibits negligible solubility in carbon dioxide at pressures below 500 atm.[37] Further, we have ignored the effects of the dispersant on the volumetric behavior, in that it is present at very low concentrations. The total volume of the system (liters) can be expressed as

$$V = n_T^{I} V^{I} + n_T^{II} V^{II} \tag{1}$$

where n_T^{I} and n_T^{II} are the total number of moles of material in phases I and II and V^{I} and V^{II} are the molar volumes of the phases, which are defined as

$$V^{I} = x_1^{I} V_1 + x_2^{I} V_2 + \Delta V_m^{I} \tag{2}$$

$$V^{II} = x_1^{II} V_1 + x_2^{II} V_2 + x_3^{II} V_3 + \Delta V_m^{II} \tag{3}$$

where the x_i's are mole fractions, the V_i's are the molar volumes of the pure components, and the ΔV_m's are the volume change upon mixing terms (i.e., the nonideal contributions to the total volume) for each phase.

Equation 1 is then differentiated as follows:

$$\{dV/dn_3^{II}\} = d\{n_T^I V^I + n_T^{II} V^{II}\}/dn_3^{II} \quad (4)$$

where eqs 2 and 3 are employed for V^I and V^{II}. Given that the V_i's are functions of temperature and pressure, but not n_3^{II}, eq 4 becomes

$$\{dV/dn_3^{II}\} = \{V_1(dn_1^I/dn_3^{II} + dn_1^{II}/dn_3^{II}) + V_2(dn_2^I/dn_3^{II} + dn_2^{II}/dn_3^{II}) + V_3 + d(n_T^I \Delta V_m^I + n_T^{II} \Delta V_m^{II})/dn_3^{II}\} \quad (5)$$

The various dn_i^j/dn_3^{II} terms reflect the change in composition of the two phases, both due to formation of polymer and transfer of CO_2 and monomer between phases as the polymerization proceeds. Owing to the high rate of mass transfer in a CO_2-based mixture, the small size of the polymer particles, and the high-intensity mixing, we assume that equilibrium is quickly established in this system. Now, given that we are running a batch system where the total number of moles of carbon dioxide is a constant:

$$dn_1^I/dn_3^{II} = -dn_1^{II}/dn_3^{II} \quad (6)$$

Likewise, $(n_2^I + n_2^{II} + n_3^{II})$ equals the initial number of moles of monomer charged to system, and so

$$(dn_2^I/dn_3^{II} + dn_2^{II}/dn_3^{II}) = -1 \quad (7)$$

Thus eq 5 reduces to

$$\{dV/dn_3^{II}\} = \{(V_3 - V_2) + d(n_T^I \Delta V_m^I + n_T^{II} \Delta V_m^{II})/dn_3^{II}\} \quad (8)$$

and so dn_3^{II}/dV becomes

$$dn_3^{II}/dV = \{(V_3 - V_2) + d(n_T^I \Delta V_m^I + n_T^{II} \Delta V_m^{II})/dn_3^{II}\}^{-1} \quad (9)$$

We can make use of eq 9 to derive the rate of polymerization as a function of the observed pressure drop in the system. If the rate of polymerization is conventionally expressed as the rate of disappearance of monomers, then

$$-(\text{rate}) = dn_3^{II}/dt = (dn_3^{II}/dV)(dP/dt)(dV/dP) \quad (10)$$

where dP/dt is the observed pressure drop, dn_3^{II}/dV is given by eq 9, and dV/dP is a measure of the degree of compressibility of the system and can be measured as described in a previous section. If we rearrange eq 10

$$dP/dt = -(\text{rate})/\{(dn_3^{II}/dV)(dV/dP)\} \quad (11)$$

In an ideal solution, where the ΔV_m terms would be zero, dn_3^{II}/dV would be negative, as the molar volume of the monomer is higher than that of the repeat units (the polymer is more dense than the monomer). Further, dV/dP is always negative, which means that one should observe a pressure drop in such a system as the polymerization proceeds. For nonideal solutions, the ΔV_m terms are nonzero, and thus dn_3^{II}/dV is as shown in eq 9. Evaluating the derivative of the nonideal terms gives

$$d(n_T^I \Delta V_m^I + n_T^{II} \Delta V_m^{II})/dn_3^{II} = \Delta V_m^I(dn_T^I/dn_3^{II}) + n_T^I d(\Delta V_m^I)/dn_3^{II} + \Delta V_m^{II}(dn_T^{II}/dn_3^{II}) + n_T^{II} d(\Delta V_m^{II})/dn_3^{II} \quad (12)$$

Because $dn_T^I/dn_3^{II} = -dn_T^{II}/dn_3^{II}$, eq 12 becomes

$$d(n_T^I \Delta V_m^I + n_T^{II} \Delta V_m^{II})/dn_3^{II} = (dn_T^{II}/dn_3^{II})(\Delta V_m^{II} - \Delta V_m^I) + n_T^I d(\Delta V_m^I)/dn_3^{II} + n_T^{II} d(\Delta V_m^{II})/dn_3^{II} \quad (13)$$

Previous work has shown that the volume change upon mixing is negative for the PMMA−CO_2 system,[37] and it is likely that ΔV_m for the MMA/CO_2 system is negative as well (ΔV_m is often small and negative for mixtures of low molecular weight liquids). Thus the first term on the right hand side of eq 13 could be positive or negative. If we assume that ΔV_m^I is indeed negative, then depletion of phase I of monomer (which occurs as n_3^{II} increases) would induce ΔV_m^I to move toward zero (and thus increase), suggesting that the second term on the right hand side of eq 13 is positive as well. This term could become quite significant, in that it is multiplied by n_T^I, the total number of moles in the CO_2-rich phase (because the number of moles of CO_2 is 1 order of magnitude larger than that of either monomer or repeat unit in dispersion polymerizations such as we have run, this term may dominate the nonideal terms). It is not clear at this time how the third term on the right-hand side of eq 13 will behave, yet it is apparent that the nonideal terms in eq 9 could combine to produce a positive value for dn_3^{II}/dV, which would therefore lead to a rise in pressure as the polymerization proceeded, as given by eq 11.

The volume change upon mixing, in addition to being a function of composition, will also be a function of pressure. In the PMMA−CO_2 system,[37] the volume change on mixing is large and negative at lower pressures, increases rapidly as pressure increases just above the critical point of CO_2, and then plateaus at higher pressures (although remaining negative). If ΔV_m for the MMA−CO_2 systems also increases in magnitude as pressure decreases, this would suggest a greater contribution of the nonideal terms at lower pressures.

Because the volume change on mixing will be a function of pressure, temperature, and the amount of monomer present in the system, one can use the change in pressure with time to compare the rates of polymerization of systems at constant T, P, and $[MMA]_0$ with different stabilizers. Operating the polymerization at higher pressures, where CO_2's volumetric behavior resembles that of a conventional liquid, allows one, as a first approximation, to neglect the nonideal terms and derive the rate of polymerization from the change in pressure with time. Although the polymerization is exothermic, the high mixing rate leads to efficient heat transfer, and thus a near-constant temperature. To compare the rate of polymerization when temperature, pressure, or [MMA] is varied, one must have knowledge of the variation of the ΔV_m terms as T, P, or $[MMA]_0$ are changed.

Results and Discussion

The effect of the molecular architecture (see Table 1) of the graft copolymer dispersant on the rate of polymerization, molecular weight of the PMMA obtained, particle size, and size distribution were studied. To

Table 1. Characteristics of the Graft Copolymers P(MMA$_x$-*co*-HEMA$_y$)-*g*-PFPO

dispersant	abbreviation	M_n[a] backbone	no. of graft chains	M_n graft chains
P(MMA$_{0.89}$-*co*-HEMA$_{0.11}$)$_{2500}$-*g*-K2500	2500-2-2500	2500	2	2500
P(MMA$_{0.89}$-*co*-HEMA$_{0.11}$)$_{2500}$-*g*-K5000	2500-2-5000	2500	2	5000
P(MMA$_{0.89}$-*co*-HEMA$_{0.11}$)$_{2500}$-*g*-K7500	2500-2-7500	2500	2	7500
P(MMA$_{0.83}$-*co*-HEMA$_{0.17}$)$_{2500}$-*g*-K2500	2500-4-2500	2500	4	2500
P(MMA$_{0.83}$-*co*-HEMA$_{0.17}$)$_{2500}$-*g*-K5000	2500-4-5000	2500	4	5000
P(MMA$_{0.83}$-*co*-HEMA$_{0.17}$)$_{2500}$-*g*-K7500	2500-4-7500	2500	4	7500
P(MMA$_{0.77}$-*co*-HEMA$_{0.23}$)$_{2500}$-*g*-K2500	2500-6-2500	2500	6	2500
P(MMA$_{0.77}$-*co*-HEMA$_{0.23}$)$_{2500}$-*g*-K5000	2500-6-5000	2500	6	5000
P(MMA$_{0.77}$-*co*-HEMA$_{0.23}$)$_{2500}$-*g*-K7500	2500-6-7500	2500	6	7500
P(MMA$_{0.89}$-*co*-HEMA$_{0.11}$)$_{5000}$-*g*-K2500	5000-5-2500	5000	5	2500
P(MMA$_{0.89}$-*co*-HEMA$_{0.11}$)$_{5000}$-*g*-K5000	5000-5-5000	5000	5	5000
P(MMA$_{0.89}$-*co*-HEMA$_{0.11}$)$_{5000}$-*g*-K7500	5000-5-7500	5000	5	7500
P(MMA$_{0.80}$-*co*-HEMA$_{0.20}$)$_{5000}$-*g*-K2500	5000-10-2500	5000	10	2500
P(MMA$_{0.80}$-*co*-HEMA$_{0.20}$)$_{5000}$-*g*-K5000	5000-10-5000	5000	10	5000
P(MMA$_{0.80}$-*co*-HEMA$_{0.20}$)$_{5000}$-*g*-K7500	5000-10-7500	5000	10	7500
P(MMA$_{0.80}$-*co*-HEMA$_{0.20}$)$_{8000}$-*g*-K2500	8000-16-2500	8000	16	2500
P(MMA$_{0.80}$-*co*-HEMA$_{0.20}$)$_{8000}$-*g*-K5000	8000-16-5000	8000	16	5000

[a] Determined by GPC and molecular weight of the backbone; the number of OH groups per backbone is known, and thus the total number of graft chains.

what extent any of the architectural attributes influenced the results depended on the nature of the variations in architecture being considered, i.e. graft chain length, graft chain density, backbone length and overall graft chain distribution. The molar composition of the starting copolymer (poly(MMA$_x$-*co*-HEMA$_y$)) was determined by ^{1}H-NMR from the relative intensities of the methylene protons of the CH_2OH of HEMA to the sum of the methylene protons of the CH_2CH_2OH of HEMA and the methyl protons of the OCH_3 group of MMA. Knowing the copolymer composition and molecular weight of the backbone, the number of OH groups per backbone was calculated; thus the total number of graft chains is known, assuming near 100% extent of reaction with PFPO−acid chloride. Table 1 indicates the backbone lengths, graft chain lengths, and the number of graft chains for each compound.

Evaluation of the Rate of Polymerization at High Pressure. As mentioned above, at high pressures we expect the nonideal mixing terms to be relatively insignificant, and thus we can evaluate the rate of polymerization directly from the change in pressure with time. The change of volume of MMA upon polymerization is available from the literature,[25] the ideal value of dn_3^{II}/dV for the system MMA−PMMA is 0.046 mol/cm^3. The value of dP/dt was calculated from the pressure readings recorded during the polymerization. The compressibility terms (dV/dP) were derived from pressure/volume measurements, as explained in the experimental section (see Figure 3). At high pressures (greater than 220 bar), the difference in the compressibility (dV/dP) between monomer−CO_2, polymer−CO_2, and monomer−polymer−CO_2 are not statistically significant, although there is a larger divergence at lower pressures. Consequently, at pressures above 220 bar, the following relationship between dV/dP and pressure was employed:

$$\frac{dV}{dP} = 1.68 \times 10^{-4} P - 0.083 \qquad (14)$$

An instantaneous rate can be determined by evaluating the values of $d[M]/dt$ through eqs 9 and 10 at various pressures. The calculated values $d[M]/dt$ can be plotted against time, and typical results of the variation of the instantaneous rate with time are shown in Figure 4.

An average reaction rate can also be calculated by evaluating eq 1 at conditions (dV/dP and dP/dt) at the midpoint of the linear pressure drop region (this is valid so long as dV/dP is linear with pressure, and pressure is linear with time). For comparison of the rate of polymerization in our study, we considered the average rate values. When repeating the experiments several times under the same conditions, the rates of the

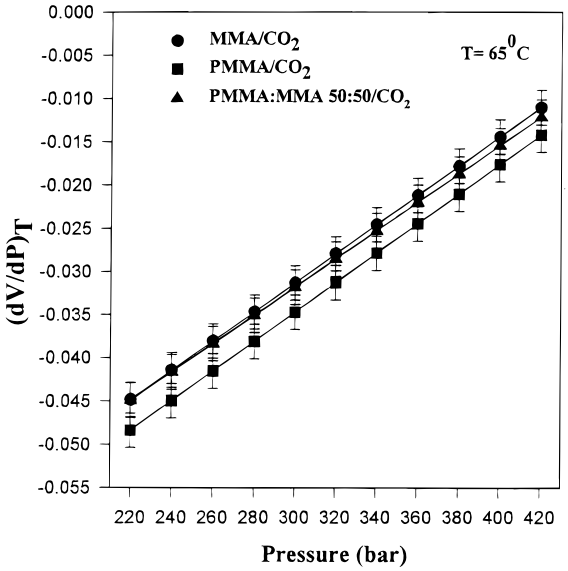

Figure 3. Compressibility of MMA−CO_2, PMMA−CO_2, and MMA−PMMA−CO_2 mixtures at 65 °C as a function of pressure.

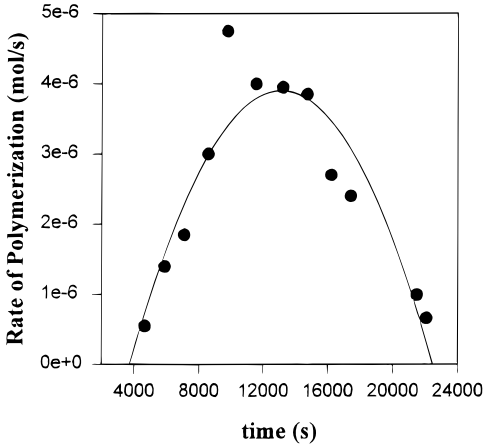

Figure 4. Example of rate of dispersion polymerization at 65 °C as a function of time.

Table 2. Effect of Dispersant Architecture on Dispersion Polymerization

dispersant	M_n, PDI[a]	mean polymerization rate (10^6 mol/s)	particle size[b] (μm)
2500-2-7500	115 000, 1.7	1.07	coagulation
2500-4-2500	52 000, 2.6	1.21	coagulation
2500-4-5000	159 000, 1.8	1.32	0.5−20 (agglomeration)
2500-4-7500	168 000, 1.7	1.66	0.5−20 (agglomeration)
2500-6-2500	116 000, 1.9	1.73	0.5−20 (agglomeration)
2500-6-5000	114 000, 2.6	2.30	0.5−20 (agglomeration)
2500-6-7500	192 000, 2.0	2.36	1−6
5000-5-2500	195 000, 1.8	2.48	1−4
5000-5-5000	200 000, 1.8	2.11	1−3
5000-5-7500	216 000, 1.8	3.77	1−1.5
5000-10-2500	278 000, 1.7	4.01	1−1.5
5000-10-5000	217 000, 1.8	2.88	1−3
5000-10-7500	230 000, 1.8	3.60	1−1.2
8000-16-2500	215 000, 1.7	1.63	2−10 (agglomeration)
8000-16-5000	355 000, 1.7	3.90	0.3−0.5

[a] Determined by GPC. [b] Determined by SEM.

reactions were found to exhibit a standard deviation of 2×10^{-7} mol/s on the rate values, which is of order $\pm 10\%$.

An approximate mass balance can be performed by approximating the area under the curve representing the change of instantaneous rate of reaction with time (see Figure 4). Approximating the rate versus time as a second-order polynomial, this technique produces a total mass of 5 g (compared to 10 g initial monomer charge), which suggests that the rate values are of the correct order of magnitude. Indeed, that the total mass did not equal 9−10 g of polymer, which was observed following polymerization runs, suggests that the non-ideal terms do play a role in eq 9, even at high pressure. However, because the ΔV_m's are functions of T, P, and $[MMA]_0$, quantities which were kept constant for these polymerizations, one can still employ dP/dt to compare relative rates of polymerization as the type and amount of dispersant is varied. For the case of the most effective stabilizers, the time required (4 h) to produce more than 90% yield of polymer compares favorably with the work of Hsiao[27] and Shaffer,[28] who each used approximately the same ratio of initiator to monomer, and approximately the same $[MMA]_0$.

Effect of Dispersant Architecture on the Dispersion Polymerization. In order to monitor the effect of dispersant architecture, the experimental conditions for monomer and initiator molar concentrations, temperature, initial pressure, and stirring rate were held constant as indicated in the Experimental Section. The dispersant molar concentration was also kept constant at 1.0 mmol/L of CO_2 for these experiments.

Other research groups have examined the effect of dispersant architecture on the dispersion polymerization of MMA in conventional liquids. For instance, El Aasser et al.[31] followed the dispersion polymerization of methyl methacrylate in methanol using linear poly(vinylpyrrolidone) or poly(vinylpyrrolidone)-*g*-poly(methyl methacrylate) (PVP-*g*-PMMA) as stabilizers. They showed that increasing the molecular weight of a linear dispersant increases the viscosity of the continuous phase and also provides better stabilization due to a higher equilibrium amount of adsorbed stabilizer. Each of these effects reduces the extent of nuclei aggregation and favors smaller particles. On the other hand, the authors showed that, in the case of a PVP-*g*-PMMA graft copolymer dispersant, an increase in the molecular weight of the anchoring component (which is soluble in methanol) increases the solubility of the surfactant in the continuous phase, resulting in a decrease in the rate of adsorption of the graft copolymer and leading to larger particles. Kumar et al.[34] studied the polymerization of methyl methacrylate in petrol using a graft copolymer, poly(methyl methacrylate-*g*-poly(12-hydroxystearic acid)), as stabilizer, with varying graft chain length. They showed that under optimal concentration conditions, as the graft chain length increases, the rate and the molecular weight of the newly formed poly(methyl methacrylate) increase. Winnik et al.[26] have followed the dispersion copolymerization of *n*-butyl methacrylate in a methanol−water mixture using a stabilizer consisting of poly(ethylene oxide) macromonomer with a *p*-alkylstyrene end group. They showed that at a given stabilizer concentration, as the alkyl chain length decreases, the particle size decreases. Matsumoto et al. followed the dispersion copolymerization of styrene in water/ethanol mixtures[29] and of methyl methacrylate in water/methanol mixtures[38] with poly(2-oxazoline) acting as a comonomer as well as the stabilizer. They showed that as the molecular weight of the macromonomer increases, the particle size decreases. Additionally, the concentration of stabilizer necessary to obtain an effective stabilization was lower than that of a conventional system since the stabilizer was chemically bonded to the forming particles. Susodiak et al.[35] found that in the case of the polymerization of methyl methacrylate in heptane, as the overall molecular weight of their triblock stabilizer isoprene-*b*-styrene-*b*-isoprene increases, the particle size decreases.

In summary, previous work has shown that the length of the anchoring group is important, as is the solubility of the dispersant in the continuous phase, although a dispersant which is too soluble will not stabilize growing particles sufficiently.

Effect of PFPO Graft Chain Length. For the series of graft copolymers with a 2500 molecular weight backbone, as the PFPO graft chain length was increased from M_n = 2500 to 7500, the average rate of the dispersion polymerization increased by 30−40% (see Table 2). Different results are observed for the two series of dispersants that contain a longer backbone (samples 5000-5-PFPO and 5000-10-PFPO). For these series, as the PFPO graft chain was increased from M_n = 2500 to 7500, the average rate of the dispersion polymerization of 5000-5-*x* increased, whereas the rate of polymerization of 5000-10-*x* actually decreases. Table 2 summarizes particle size and molecular weight data for the PMMA obtained. For backbone lengths of 2500 and 5000, the molecular weight, particle size, and size

distribution were not strongly affected by the change in the PFPO graft chain length (from M_n = 2500 to 7500). In previous work,[36] we have shown that increasing the length of graft chains increases the size of the single phase region in $P-x$ space, although the magnitude of the enahncement decreases as the total amount of fluoroether in the copolymer increases. Thus, the effect of increased tooth length on the solubility of the graft copolymers is greatest for the shortest graft chain length.

Effect of PFPO Graft Chain Density. The dispersant architecture was varied by increasing the graft chain density (the number of PFPO teeth per macromolecule). For instance, we compare the rate of the dispersion polymerization of series of samples containing a 2500 PFPO graft chain, and various PFPO graft chain densities (PFPO tooth number). As the number of PFPO teeth increases from 4 to 6, for a backbone of M_n = 2500 (samples 2500-4-2500 and 2500-6-2500), or from 5 to 10 teeth, for a backbone of M_n = 5000 (samples 5000-5-2500 and 5000-10-2500), the rate of polymerization increases by 40−60%. Similar results are obtained for samples containing longer PFPO graft chains (M_n = 5000 to 7500), although in the case of the highest molecular weight dispersants (5000-5-7500 vs 5000-10-7500), adding additional teeth leads to no increase in the rate of polymerization, and actually a slight decrease. For these high molecular weight materials, we may be approaching the limit beyond which adding CO_2-philic groups to the molecule leads to no further decrease in dispersant cloud point pressures. In general, though, for a given PFPO graft chain length, as the number of PFPO graft chains increases, the average rate of polymerization increases, a result which is probably partially dependent on the solubility of the dispersant in CO_2. As the PFPO graft chain density increases, we have shown[36] that the solubility of the graft copolymer in CO_2 increases significantly, although one eventually reaches a point of diminishing returns at high PFPO chain lengths and large numbers of teeth. Therefore, increasing the solubility of our dispersant for a given anchor group length (backbone length) in the continuous phase leads to a better stabilization of the dispersed system, which leads to faster polymerization rates.

As shown in Table 2, the molecular weight of the PMMA obtained ranges from M_n = 50 000 to 350 000 but does not appear to depend on the PFPO graft chain density (for a given backbone length). The particle size and size distribution are not strongly dependent on the PFPO graft chain density, except in those cases where little or no particle stabilization was achieved. For example, a graft copolymer containing a backbone of M_n = 2500, and four PFPO graft chains of M_n = 2500 (i.e., 2500-4-2500) per molecule did not provide sufficient stabilization, leading to coagulation and generally lower molecular weight PMMA. For these graft copolymers, it is also clear that the backbone molecular weight is an important parameter in determining the ability to stabilize growing PMMA spheres in CO_2. Once the proper backbone length is reached, increasing the graft chain density (comparing 5000-5-*x* to 5000-10-*x* behavior in Table 2, where *x* is either 2500, 5000, or 7500) reduces particle size somewhat and also narrows the particle size distribution. For a given backbone length, PMMA molecular weight, however, is relatively unaffected by graft chain density. SEM photographs are shown in Figure 5.

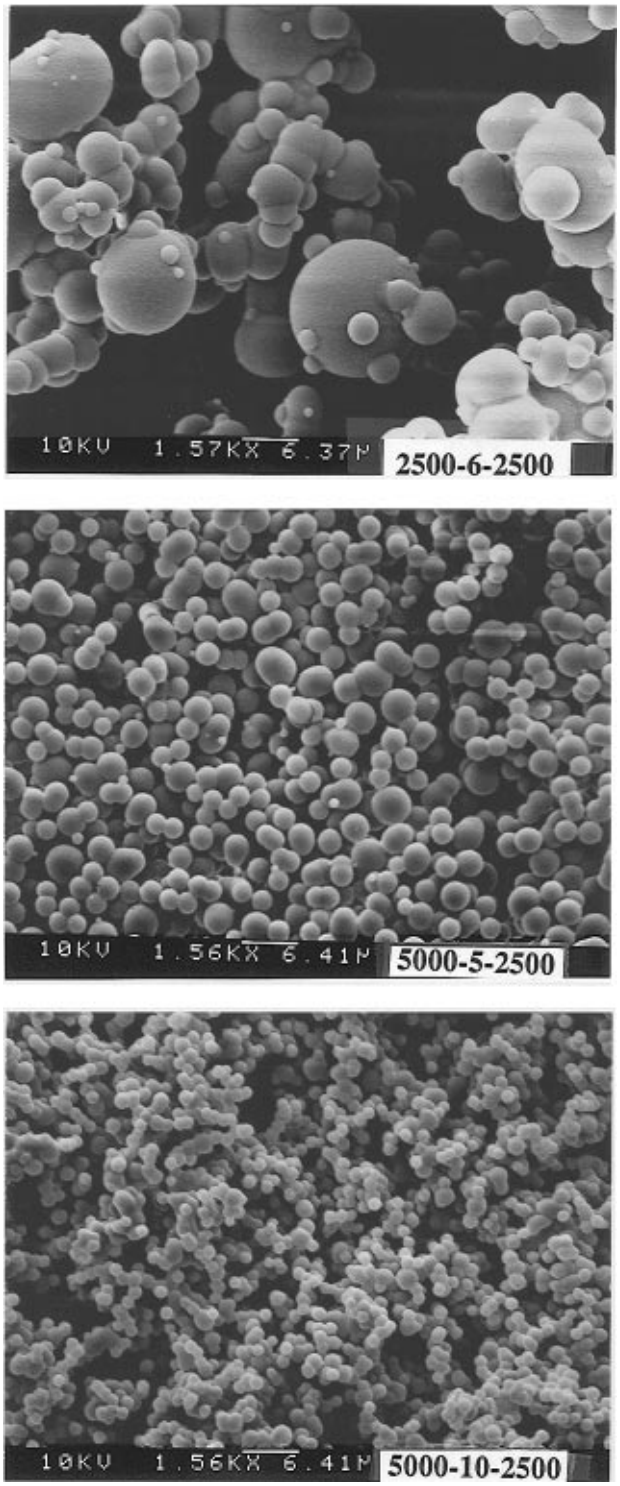

Figure 5. SEM photographs of PMMA spheres; effect of dispersant graft chain density on particle size for samples 2500-6-2500, 5000-5-2500, and 5000-10-2500.

Effect of Backbone Length. The parameter that most strongly affects rate, particle size, and size distribution was found to be the length of the backbone. The architecture was varied by increasing the molecular weight (M_n) of the backbone of the graft copolymer (P(MMA$_x$-*co*-HEMA$_y$) from M_n = 2500 to 5000 to 8000.

For a PFPO graft chain of M_n = 2500, as the overall architecture is doubled (i.e., compare 2500-6-2500 to 5000-10-2500), the average rate of polymerization is increased by 130%. On the other hand, as the overall size of the copolymer is further increased (8000-16-2500), the average rate of polymerization drops drasti-

cally (by 150%) and complete agglomeration of the PMMA particles is observed. These results show that a certain length of the backbone or anchoring component is necessary to achieve efficient polymerization, but that is not the only essential parameter. In addition to the anchor group size, the dispersant must contain enough CO_2-philic groups (PFPO) to ensure solubilization in the continuous phase. In this case, 20 mol % of PFPO graft chains of $M_n = 2500$ (i.e., 16 teeth of $M_n = 2500$) are not sufficient to provide solubilization of the graft copolymer with a backbone of $M_n = 8000$ (a cloudy medium is observed after loading the reactor, indicating the presence of an insoluble component in CO_2). This leads to slow polymerization and particle agglomeration. To confirm these results, another dispersant employing longer PFPO graft chains was synthesized, in order to achieve better solubility of the graft copolymer in CO_2. As the results in Table 2 show, for PFPO graft chains of $M_n = 5000$, as the overall architecture of the dispersant is doubled (dispersant 5000-10-5000 compared to 2500-6-5000) or tripled (dispersant 8000-16-5000 compared to 2500-6-PFPO), the average rate of polymerization nearly doubles. As the backbone length increases, if the dispersant possesses enough CO_2-philic groups to assure complete solubility in the continuous phase, the anchoring and surface coverage of the growing particles is improved, which lead to an increase in the rate of polymerization.

As shown in Table 2, the particle size and size distribution decrease steadily as the backbone length increases, provided that enough CO_2-philic component has been included. Micron-size particles are obtained in the case of the graft copolymer containing a backbone of $M_n = 5000$, 20 mol % of PFPO graft chains of $M_n = 2500-7500$ (SEM pictures are shown in Figure 6). Submicron PMMA beads are obtained in the case of dispersant 8000-16-5000. In general, the molecular weight of the PMMA obtained increases as the backbone molecular weight increases.

An additional experiment was performed to check if either the surface coverage (i.e., the actual weight fraction of dispersant) or the adsorption capability of the dispersant (i.e., the actual length of the backbone or anchor group) plays the more important role in particle stabilization. Results for 2 mmol/L of CO_2 of dispersant 2500-6-2500 were compared to 1 mmol/L of CO_2 of dispersant 5000-10-2500. As illustrated in Table 3, by doubling the concentration (to provide a larger surface coverage), the rate of polymerization was similar to one obtained using the larger molecule. However, the particle size and size distribution are not similar for the two cases: a longer backbone gives smaller particles with a narrower size distribution. We can conclude that a longer backbone provides not only a better surface coverage but also a better anchoring of the dispersant, which will eventually control the particle size and size distribution and will not equal results obtained by just increasing the weight basis of a dispersant with a smaller anchoring group.

From these results, we can conclude that the backbone length is a key component to achieve the best conditions for the dispersion polymerization (particle size and rate). By increasing the backbone length, i.e. the anchor length, a better stabilization is achieved by a better anchorage and surface coverage of the growing polymer particles, which is further indicated by faster polymerization rate and smaller particles. But a careful balance between the anchor and soluble component is essential if the dispersant is to function efficiently.[25] If the anchor/soluble balance leans toward the anchor group, the dispersant will exist predominantly as ag-

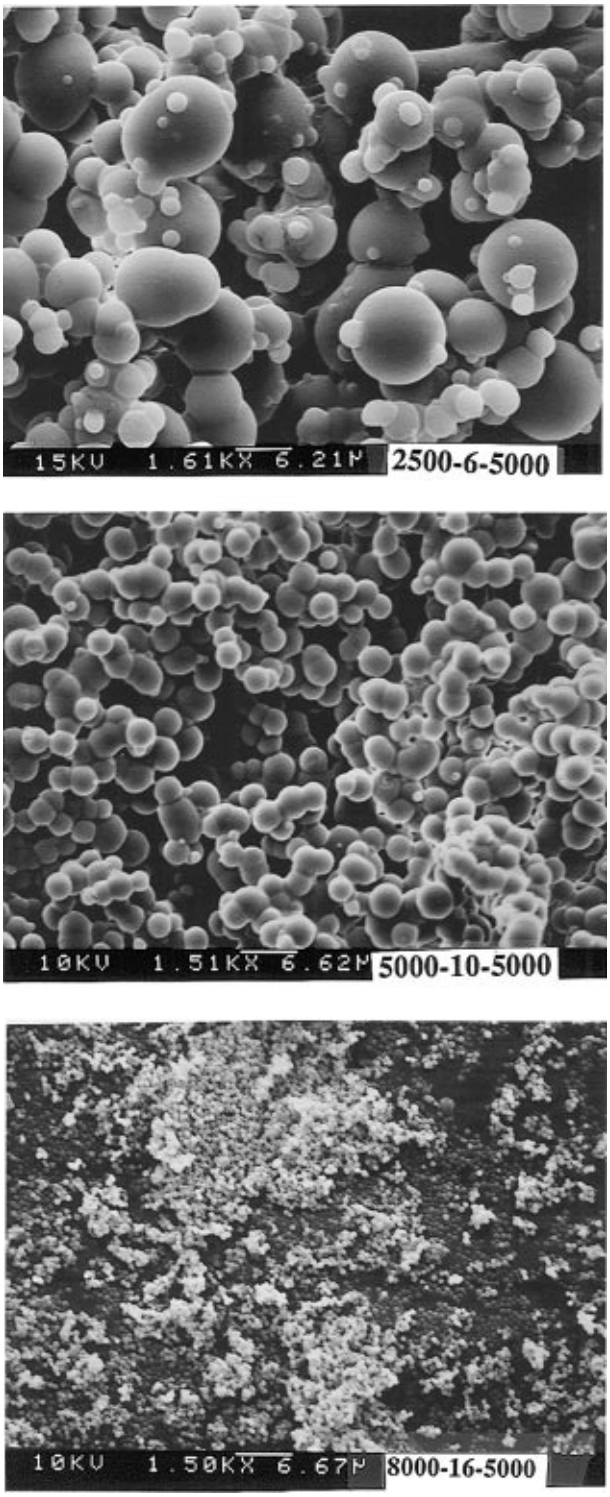

Figure 6. SEM photographs of PMMA spheres; effect of dispersant backbone length on particle size for samples 2500-6-5000, 5000-10-5000, and 8000-16-5000.

Table 3. Effect of Backbone Length on Dispersion Polymerization

dispersant	concn (mmol/L of CO_2)	rate (10^6 mol/s)	particle size[b] (μm)	M_n, PDI[a]
5000-10-2500	1.0	4.01	1−1.5	224 000, 1.8
2500-5-2500	2.0	3.46	1−8	278 000. 1.7

[a] Determined by GPC. [b] Determined by SEM.

Table 4. Effect of Distribution of Fluoroether Groups in Graft Copolymers on Dispersion Polymerization of MMA

dispersant	M_n, PDI[a]	mean polymerization rate (10^6 mol/s)	particle size[b] (μm)
2500-2-7500	115 000, 1.7	1.07	coagulation
2500-6-2500	116 000, 1.7	1.73	0.5−20 (agglomeration)
5000-5-5000	200 000, 1.8	2.11	1−3
5000-10-2500	278 000, 1.7	4.01	1−1.5

[a] Determined by GPC. [b] Determined by SEM.

gregates which will not dissociate easily or will not be soluble enough in the continuous phase and hence will not sufficiently stabilize the particles, as we have observed for the dispersant 8000-16-2500. On the other hand, if the anchor group is too small, the dispersant will be freely soluble and will tend to remain in the continuous phase. It will not adsorb and readily cover the growing particle surface, thus enabling efficient stabilization, as we have observed for the dispersant 2500-2-7500.

Graft Chain Distribution. The data in Table 4 show the effect of graft chain architecture on the dispersion polymerization. The rate of polymerization is compared for several series of graft copolymers whose PFPO graft chain distribution is varied. One series compares a sample containing 11 mol % of PFPO graft chains of $M_n = 5000$ (i.e., 5000-5-5000) to one containing 20 mol % of PFPO graft chains of $M_n = 2500$ (i.e., 5000-10-2500). Both samples contain the same backbone molecular weight ($M_n = 5000$). In each case, although containing the same amount of fluoroether per backbone unit (same balance of soluble/anchor groups), the samples exhibit very different rates of polymerization, particle size, and size distribution. The sample with shorter and more numerous teeth (5000-10-2500) has an average rate of polymerization twice as large as the sample with fewer longer teeth (5000-5-5000). Additionally, 1 μm beads with low size distribution are obtained with the dispersant 5000-10-2500. Similar results are obtained for another series of dispersant, i.e., comparing dispersant 2500-2-7500 to 2500-6-2500. No stabilization was achieved in the case of dispersant 2500-2-7500, where complete coagulation was observed. Hence, these results show that it is important not only how long the backbone is and what fraction of the dispersant is CO_2-philic but also how the CO_2-philic part of the dispersant is distributed along the backbone.

Effect of Initial Pressure on the Dispersion Polymerization. The effect of initial pressure of the reaction medium on the rate of polymerization, particle size and size distribution, and polymer molecular weight was observed. All variables except pressure, such as the monomer and initiator molar concentration, temperature, and stirring rate were held constant as indicated in the Experimental Section. The dispersant molar concentration was kept constant at 1.0 mmol/L of CO_2 in all experiments. Two different dispersants were chosen for this study, 5000-10-2500 and 5000-5-2500, in order to check the reproducibility of the results and compare the results in the case of a "good" stabilizer and an "average" one. The results are summarized in Tables 5 and 6.

In the case of the dispersant 5000-10-2500, five reactions were carried out at initial pressures ranging from 380 to 90 bar, thus including pressures above and below the cloud point pressure of the pure dispersant. As the initial pressure was reduced from 380 to 241 bar, the overall pressure drop observed upon polymerization decreased in absolute value, as did the rate of pressure decrease. When the reaction was carried out with an initial pressure of 172 bar, an increase of the overall pressure of the system upon polymerization was observed (instead of the usual pressure decrease), even under the isothermal conditions employed. A similar pressure increase was observed at 90 bar, and the overall pressure change increased in absolute value. In all cases, dry polymer powder was collected after the reaction was completed. The SEM pictures obtained are illustrated in Figure 7. As the initial pressure decreases, the solubility of the dispersant in CO_2 decreases, which manifests itself as an agglomeration of 1 μm beads at 310 and 241 bar, in comparison with the results at 380 bar. By further decreasing the initial pressure (to 172 and 90 bar), the particles coalesce in larger units, forming a "macrostructure". These units also increase in size as the initial pressure, or dispersant solubility, is decreased (units of ca. 7 μm at 172 bar and 20 μm at 90 bar), as shown in Figure 7.

Table 5. Initial Pressure Effect on Dispersion Polymerization Using the Stabilizer 5000-10-2500

initial pressure (bar)	overall pressure change (bar)	rate of pressure drop (bar/min)	particle size[b] (μm)	M_n, PDI[a]
380	−48	−0.289	1−1.5	278 000, 1.7
310	−24	−0.165	0.7−1 (agglomeration)	280 000, 1.6
241	−17	−0.193	0.7−1 (agglomeration)	215 000, 1.7
172	+20	+0.103	7 to clumps	250 000, 1.8
90	+28	+0.179	20 to clumps	268 000, 1.7

[a] Determined by GPC. [b] Determined by SEM.

Table 6. Initial Pressure Effect on Dispersion Polymerization Using the Stabilizer 5000-5-2500

initial pressure (bar)	overall pressure drop (bar)	rate of pressure drop (bar/min)	particle size[b] (μm)	M_n, PDI[a]
400	−62	−0.214	1−4	195 000, 1.8
275	−13	−0.031	1−1.5 (agglomeration)	237 000, 1.6
193	+21	+0.152	coagulation	187 000, 1.8

[a] Determined by GPC. [b] Determined by SEM.

Similar results are observed for the stabilizer 5000-5-2500, as shown in Table 6. As the initial pressure is decreased, the solubility of the dispersant in CO_2 decreases. Initially, this translates to a reduction in the overall pressure drop upon polymerization, but eventually a pressure increase is observed, and the agglomeration of small particles in larger units results. PMMA molecular weight, however, is relatively unaffected by variation of the initial pressure of polymerization.

As shown in a previous section, whether the pressure rises or falls during polymerization depends upon the magnitude of the nonideal mixing terms, particularly the excess volume of the monomer−CO_2 mixture, which contributes to the sign of the term dn_3^{II}/dV in eq 9. Not surprisingly, as the pressure drops these nonideal terms become more important (at high pressures, the compressibility of CO_2 drops and it exhibits more liquid-like behavior), leading to a change in sign of dP/dt during polymerization. Because we do not at present know how the ΔV_m terms depend upon pressure and composition, we cannot use the dP/dt's obtained at different pressures to calculate rates for these runs. It is interesting that one can obtain a dry polymer powder of significant molecular weight at pressures as low as 90 bar, despite the fact that this is well below the cloud

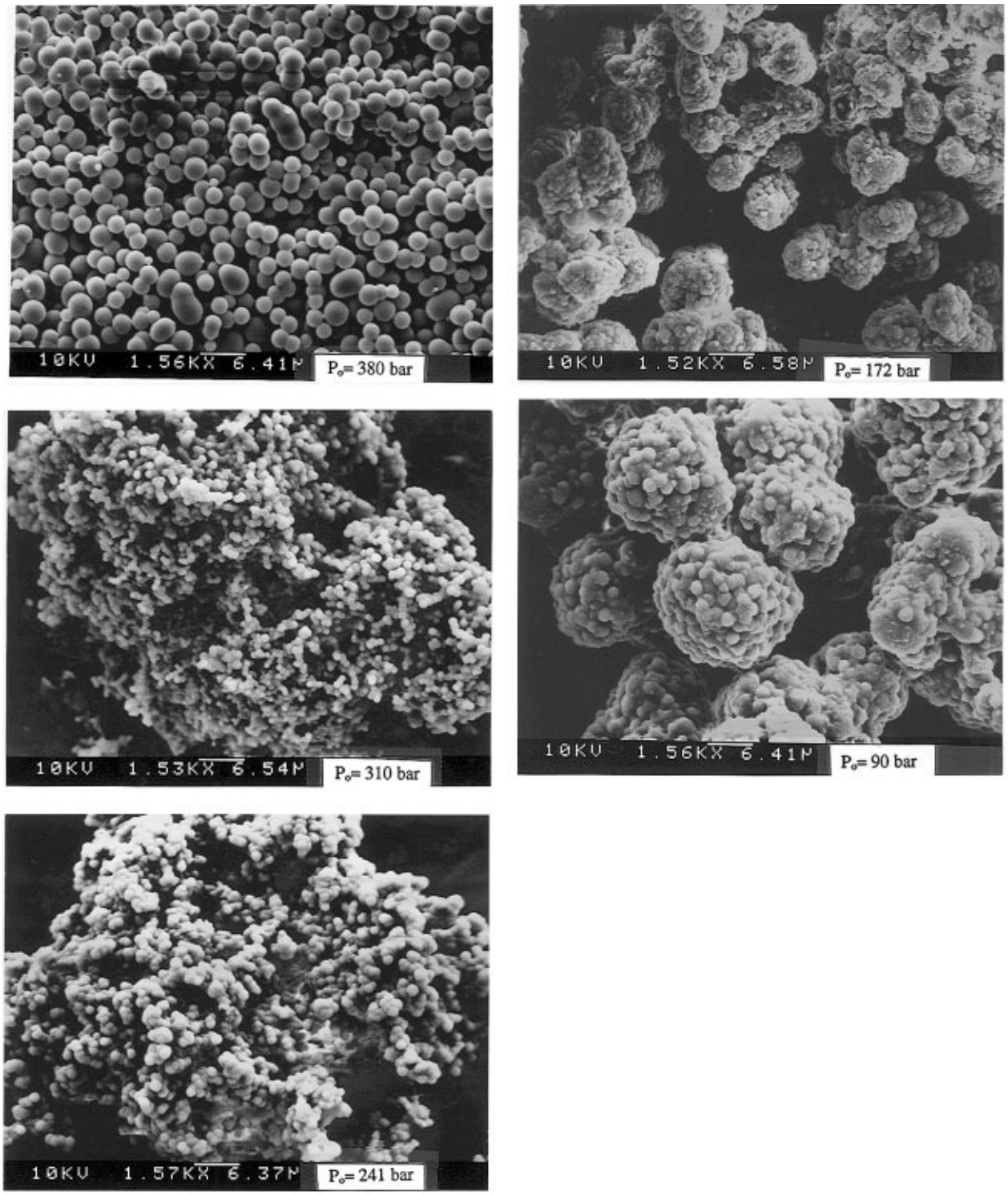

Figure 7. SEM photographs of PMMA spheres; effect of initial pressure on particle size, using dispersant 5000-10-2500.

point pressure of the dispersant in CO_2. It should be noted that the continuous phase (at least initially) is a mixture of CO_2 and MMA, whose solvent strength is significantly greater than that of CO_2 alone, which apparently allows formation of high molecular weight material (although in large aggregates) at such low pressures.

Effect of Stabilizer Concentration. The effect of stabilizer concentration on polymerization rate, particle size and size distribution, and polymer molecular weight was investigated for two different dispersants: 5000-5-7500 and 2500-6-5000. The experimental conditions for monomer and initiator molar concentrations, temperature, initial pressure, and stirring rate are those indicated in the Experimental Section. The results are summarized in Table 7 and Figure 8.

In the case of the dispersant 5000-5-7500, the molar concentration is varied from 0.5 to 1.5 mmol/L of CO_2 (i.e. from 2 to 5 wt %). Figure 8 shows the variation of the average rate of polymerization with dispersant concentration, which increases as the dispersant concentration is increased up to about 0.8 mmol/L of CO_2 and then decreases when the concentration is further increased. That the rate goes through a maximum at a certain concentration has been reported in the literature[25,32,33] and has been explained in terms of mass

Table 7. Effect of Dispersant Concentration on Dispersion Polymerization Using Stabilizer 5000-5-7500

[dispersant] (mmol/L of CO_2)	M_n, PDI[a]	particle size (μm)
0.52	265 000, 1.7	2−2.5 (agglomeration)
0.78	275 000, 1.7	1.8−2 (agglomeration)
1.0	216 000, 1.8	1−2
1.5	400 000, 1.6	0.8−1

[a] Determined by GPC. [b] Determined by SEM.

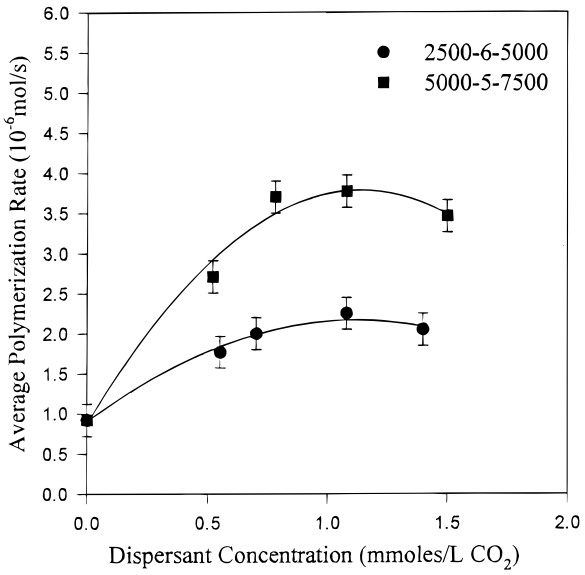

Figure 8. Effect of dispersant concentration on polymerization rate for samples 5000-5-7500 and 2500-6-5000.

transfer arguments. As the concentration of the dispersant reaches a certain value, the rate of diffusion of monomers toward the locus of polymerization is hindered, which leads to a decrease in the polymerization rate. Further, as illustrated by the SEM shown in Figure 9, the particle size and size distribution decrease as the dispersant concentration increases, which confirms results shown by the literature. Submicron beads were obtained in the case where the dispersant concentration was 1.5 mmol/L of CO_2.

In the case of 2500-6-5000, similar results are obtained when the concentration is varied from 0.55 to 1.7 mmol/L of CO_2 (i.e., from 1.6 to 5 wt %). As Figure 8 shows, the average rate of polymerization increases slightly as the dispersant concentration increases (over the range of concentration studied). In the case of 0.55 mmol/L of CO_2, relatively poor stabilization was achieved, leading to a low rate of polymerization and coagulated particles. From SEM measurements, typical particle sizes obtained ranged from 0.5 to 20 μm with a broad particle size distribution, over the concentration range. The overall particle size and size distribution started to decrease as the concentration reached 1.7 mmol/L of CO_2. No trend was observed for the effect of dispersant concentration on the molecular weight of PMMA, over the range of concentration studied.

Conclusions

Our results show that a careful balance between the size of the anchor group (backbone length) and the amount of the soluble component (either graft chain length or the graft chain density) is necessary but not sufficient in order to achieve the best stabilization condition. How the soluble component is distributed along the anchor group has also been shown to play an important role. If the balance leans toward the soluble component, the dispersant will be more soluble in the continuous phase and show a poorer adsorption onto the particle surfaces, leading to larger particle size and size distribution. On the other hand, if the balance leans toward the anchor group (backbone length), the adsorption onto the particle surface is improved, leading to smaller narrow disperse particles and a larger molecular weight polymer. But it seems important that the solubility of the dispersant in the continuous phase be sufficiently good; otherwise the dispersant will not facilitate the necessary stabilization, thus leading to a larger particle size and size distribution. The best

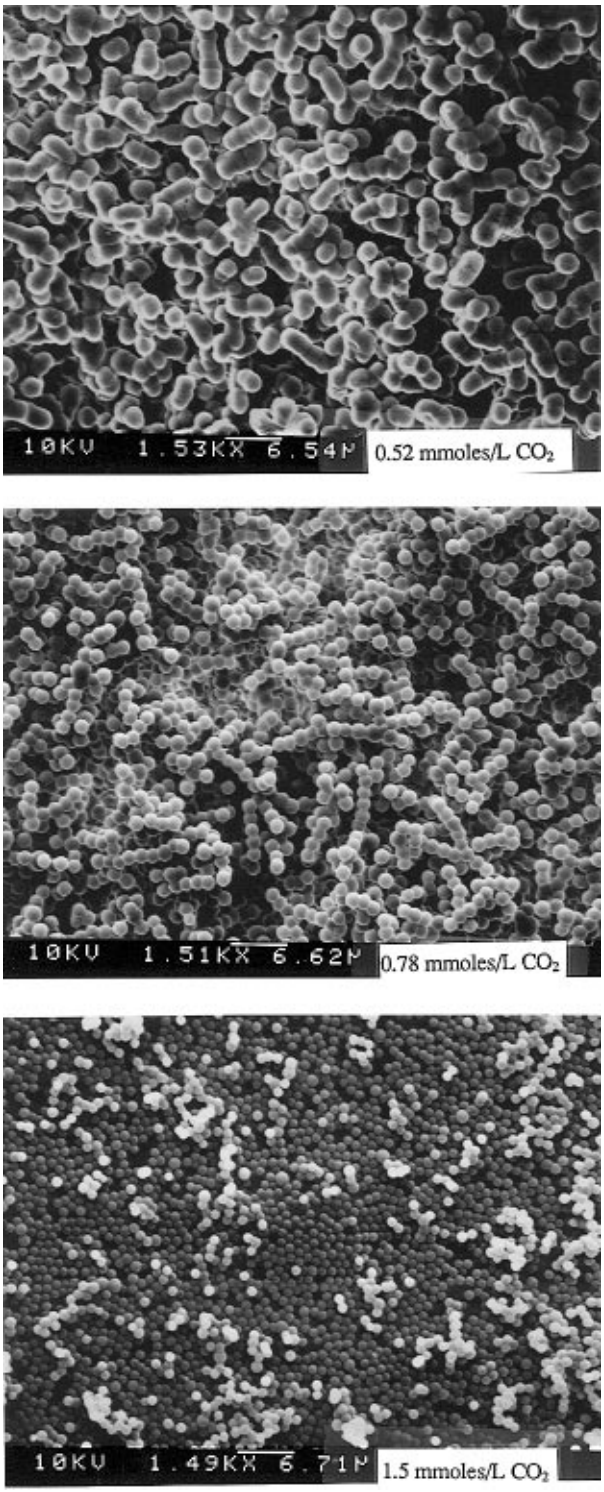

Figure 9. SEM photographs of PMMA spheres; effect of stabilizer concentration on particle size.

stabilization conditions can be achieved at a pressure where the dispersant is soluble enough to assure non-agglomeration. Additionally, an optimal concentration for each dispersant structure can be found in order to provide sufficient surface coverage (yet without hindering monomer diffusion toward the locus of polymerization) leading to submicron PMMA beads.

Acknowledgment. The authors wish to thank Marie W. Urick of Bayer Corp. for her assistance with the scanning electron microscopy and the National Science Foundation (CTS-9258580) for financial support.

References and Notes

(1) McLaren, L.; Myers, M. N.; Giddings, J. C. *Science* **1968**, *159*, 197.
(2) Myers, N. M.; Keller, R. A.; MacLaren, L. *Science* **1968**, *162*, 67.
(3) Randolph, T. W.; Clark, D. S.; Blanch, H. W.; Prausnitz, J. M. *Science* **1988**, *238*, 387.
(4) Russell, A.; Beckman, E. J. *J. Appl. Biochem. Biotechnol.* **1991**, *31*, 197.
(5) Scholsky, K. M. *Polym. Prepr. (Am. Chem. Soc., Div. Polym. Chem.)* **1990**, *31*, 685.
(6) Hubert, P. *Angew. Chem., Int. Ed. Engl.* **1978**, *17*, 710.
(7) Subramanian, B.; McHugh, M. A. *Ind. Eng. Chem. Process Res. Dev.* **1986**, *26*, 1.
(8) Guan, Z.; Combes, J. R.; Elsbernd, C. S.; DeSimone, J. M. *Polym. Prepr. (Am. Chem. Soc., Div. Polym. Chem.)* **1993**, *34* (1), 447.
(9) Hunt, M. O.; Belu, A. M.; Linton, R. W.; DeSimone, J. M. *Polym. Prepr. (Am. Chem. Soc., Div. Polym. Chem.)* **1993**, *34* (1), 445.
(10) Combes, J. R.; Guan, Z.; DeSimone, J. M. *Macromolecules* **1994**, *27*, 865.
(11) Lole, A. K.; Shine, A. D. *Polym. Prepr. (Am. Chem. Soc., Div. Polym. Chem.)* **1990**, *31*, 677.
(12) Iezzi, A.; Bendale, P.; Enick, R. M.; Turberg, M.; Brady, J. *Fluid Phase Equilib.* **1989**, *52*, 307.
(13) Francis, A. W. *J. Phys. Chem.* **1954**, *58*, 1099.
(14) McFann, G. J.; Johnston, K. P.; Hurter, P. N.; Hatton, T. A. *Ind. Eng. Chem. Res.* **1993**, *32*, 2336.
(15) Consani, K. A.; Smith, R. D. *J. Supercrit. Fluids* **1990**, *3*, 51.
(16) DeSimone, J. M.; Guan, Z.; Elsbernd, C. S. *Science* **1992**, *257*, 945.
(17) Guan, Z.; Combes, J. R.; Menceloglu, Y. Z.; DeSimone, J. M. *Macromolecules* **1993**, *26*, 2663.
(18) DeSimone, J. M.; Maury, E. E.; Mencelogu, McClain, J. B.; Romack, T. J.; Combes, J. R. *Science* **1994**, *265*, 356.
(19) Dandge, D. K.; Heller, J. P.; Wilson, K. V. *Ind. Eng. Chem. Prod. Res. Dev.* **1985**, *24*, 162.
(20) Hoefling, T. A.; Newman, D. A.; Enick, R. M.; Beckman, E. J. *J. Supercrit. Fluids* **1993**, *6*, 165.
(21) Newman, D. A.; Hoefling, T. A.; Beitler, R. R.; Beckman, E. J.; Enick, R. M. *J. Supercrit. Fluids* **1993**, *6*, 205.
(22) Tuminello, W. H.; Dee, G. T.; McHugh, M. A. *Macromolecules* **1995**, *28*, 1506.
(23) Romack, T. J.; Combes, J. R.; DeSimone, J. M. *Polym. Prepr. (Am. Chem. Soc., Div. Polym. Chem.)* **1995**, *36* (1), 509.
(24) Hoefling, T. A.; Stofesky, D.; Reid, Beckmann, E. J.; Enick, R. M. *J. Supercrit. Fluids* **1992**, *5*, 237.
(25) Barett, K. E. J. *Dispersion polymerization in organic media*; Wiley & Son: London, 1976.
(26) Kawaguchi, S.; Winnik, M.; Ito, K. *Macromolecules* **1995**, *28*, 1159.
(27) Hsiao, Y.-L.; Maury, E. E.; DeSimone, J. M.; Mawson, S.; Johnston, K. P. *Macromolecules* **1995**, *28*, 8159.
(28) Shaffer, K. A.; Jones, T. A.; Canelas, D. A.; DeSimone, J. M.; Wilkinson, S. P. *Macromolecules* **1996**, *29*, 2704.
(29) Kobayashi, S.; Uyama, H.; Won Lee, S.; Matsumoto, Y. *J. Polym. Sci., Part A: Polym. Chem.* **1993**, *31*, 3133.
(30) Odian, G. *Principles of Polymerization*, 3rd ed.; Wiley-Interscience: New York, 1995.
(31) Shen, S.; Sudol, E. D.; El-Aasser, M. S. *J. Polym. Sci., Part A: Polym. Chem.* **1994**, *32*, 1087.
(32) Uyama, H.; Kobayashi, S. *Polym. Int.* **1994**, *34*, 339.
(33) Kobayashi, S.; Uyama, H.; Yamamoto, I.; Matsumoto, Y. *Polym. J.* **1990**, *22*, 759.
(34) Kargupta, K.; Rai, P.; Kumar, A. *J. Appl. Polym. Sci.* **1993**, *49*, 1309.
(35) Susodiak, O.; Barton, J. *J. Chem. Pap.* **1985**, *39*, 379.
(36) Lepilleur, C.; Beckman, E. J.; Schoenemann, H.; Krukonis, V. J. *Fluid Phase Equilib.*, in press.
(37) Beckman, E. J. Thermodynamics of Supercritical Gas-Polymer Mixtures. Ph.D. Thesis, 1988.
(38) Kobayashi, S.; Uyama, H.; Choi, J. H.; Matsumoto, Y. *Polym. Int.* **1993**, *30*, 265.

MA960764S